Coactivator Assembly at the Promoter: Efficient Recruitment of SRC2 Is Coupled to Cooperative DNA Binding by the Progesterone Receptor †

ARTICLE *in* BIOCHEMISTRY · NOVEMBER 2007

Impact Factor: 3.02 · DOI: 10.1021/bi700850v · Source: PubMed

BIOCHEMISTRY

 Volume 46, Number 39 October 2, 2007

Articles

Coactivator Assembly at the Promoter: Efficient Recruitment of SRC2 Is Coupled to Cooperative DNA Binding by the Progesterone Receptor†

Aaron F. Heneghan,‡ Keith D. Connaghan-Jones,‡ Michael T. Miura, and David L. Bain*

Department of Pharmaceutical Sciences, University of Colorado Health Sciences Center, 4200 East 9th Avenue, Denver, Colorado 80262

Received May 4, 2007; Revised Manuscript Received June 19, 2007

ABSTRACT: A largely unsolved problem in eukaryotic gene regulation focuses on the mechanisms by which DNA-bound transcription factors recruit coactivators to a promoter. Recent work has suggested that promoter DNA acts as an allosteric ligand, serving not only to bind and localize transcription factors but also to trigger structural changes within the proteins in order to elicit coactivator recruitment. Unfortunately, a quantitative and molecular understanding of this phenomenon remains unclear. We have previously resolved the microstate interaction energetics of progesterone receptor A-isoform (PR-A) assembly at multiple promoters; here we extend this work to the role of PR-A in mediating promoter-dependent recruitment of the coactivator, SRC2. Quantitative footprinting and statistical thermodynamic modeling of PR-A:promoter interactions in the presence and absence of coactivator demonstrate that receptor binding to a single response element is maximally coupled to a 2-fold enhancement in SRC2 binding. By contrast, PR-A assembly at multiple response elements is linked to an additional 6- to 10-fold increase in SRC2 affinity. This effect arises due to a coupled reaction between SRC2 uptake and enhanced cooperative interactions between adjacently bound PR-A dimers. Put another way, increased coactivator levels stabilize a higher-order receptor−promoter complex. These results may thus not only offer a mechanism for explaining the weak transcriptional activity seen for promoters containing a single binding site and the synergistically strong activity seen for multisite promoters but also suggest that *in vivo* fluctuations of coactivator levels might serve as a physiological regulator of assembly for PR-A (and for other nuclear receptors) at the promoter.

Progesterone receptors (PR) are members of the nuclear receptor superfamily of ligand-activated transcription factors (*1*). As a general rule, receptors such as PR function by binding to response elements at upstream promoter sites and recruiting an array of coactivating proteins. These reactions are coupled to interactions with the general transcriptional activation machinery and thus increased gene transcription. The exact basis by which receptors recruit coactivators remains elusive, particularly when considered in the context of chromatin structure. However, it is well accepted that the promoter DNA can act as an allosteric ligand (*2*), serving not only to bind and localize the receptors to the promoter but also to trigger structural changes within the proteins in order to elicit coactivator recruitment.

† This work was supported by grants from the National Institutes of Health (R01-DK061933 to D.L.B. and F32-DK070519 to A.F.H.) and a grant from the American Association of the Colleges of Pharmacy (D.L.B.).

* To whom correspondence should be addressed: Department of Pharmaceutical Sciences, C-238, University of Colorado Health Sciences Center, 4200 E. 9th Ave., Denver, CO 80262. Phone: 303-315-1416. Fax: 303-315-0274. E-mail: David.Bain@UCHSC.edu.

‡ These authors contributed equally to this work.

10.1021/bi700850v CCC: $37.00
Published on Web 09/11/2007

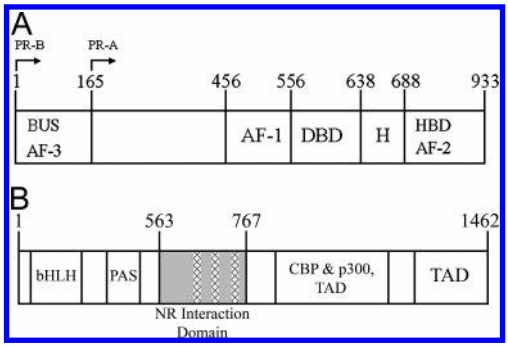

FIGURE 1: Progesterone receptor and SRC2 domain structures. (A) Schematic of primary amino acid sequence for PR-A and PR-B isoforms. Functional regions are as indicated: DBD, DNA binding domain; HBD, hormone binding domain; H, hinge; AF, activation function; BUS, B-unique sequence. PR-B is defined as amino acids 1−933; PR-A is defined as amino acids 165−933. (B) Schematic of primary amino acid sequence for SRC2. Functional regions are as indicated: bHLH, basic helix loop helix; PAS, Per-ARNT-SIM region; CBP and P300, binding site for CREB binding protein and p300 protein; TAD, trans-activation domain. Amino acids 563−767 correspond to the nuclear receptor interaction domain used in these studies. The three cross hash regions within the nuclear receptor interaction domain correspond to the three LXXLL motifs.

As shown in Figure 1A, PR exists naturally as two isoforms, PR-A and PR-B. Both isoforms are identical with the exception that PR-A is lacking 164 amino acids at its N-terminus. The two proteins share in common a centrally localized DNA binding domain (DBD), a C-terminal hormone binding domain (HBD), and transcriptional activation functions (AFs) 1 and 2. Within the 164 residue B-unique sequence (BUS) is located a context-dependent AF-3 (*3*, *4*). Despite their near identity, the two isoforms maintain a number of distinct functional differences (*5*−*9*). In particular, PR-B has historically been found to be a stronger transcriptional activator than PR-A at promoters containing multiple progesterone response elements (PREs), although both isoforms are trancriptionally weak on promoters containing a single PRE (*10*). More recent microarray analyses have revealed that the isoforms regulate different subsets of genes, and that isoform-specific transcriptional activity can vary greatly (*9*). The basis by which these differences occur remains unclear.

One class of coactivators responsible for PR-mediated transcriptional activation is the p160 or steroid receptor coactivator (SRC) family (*11*). Seen in Figure 1B is the schematic layout of the coactivator, SRC2 (*12*). The protein is made up of a number of functional units, including an N-terminal basic helix−loop−helix Per-ARNT-SIM region (bHLH-PAS), a centrally located nuclear receptor interaction domain (NRID), and multiple C-terminal transcriptional activation domains (TADs) capable of interacting with histone acetyltransferases such as p300 and CBP. The 21 kDa NRID sequence contains three LXXLL motifs demonstrated by structural and functional analyses to interact with nuclear receptor ligand binding domains (including the LBDs of PR) in a manner thought to be comparable to its full-length counterpart (*13*, *14*).

Our previous work on the thermodynamics of PR isoform−promoter interactions revealed that both isoforms were able to bind cooperatively to promoters containing multiple PREs with high affinity (*15*, *16*). However, residues unique to PR-B served to allosterically modulate the assembly energetics in such a way as to enhance PR-B binding affinity relative to PR-A. As a consequence, the differences in microscopic binding energetics predicted receptor−promoter occupancies that accurately correlated with the transcriptional activation profiles seen for each isoform. These results made it unnecessary to invoke *a priori* differential recruitment of coactivators as the basis for explaining the differences in isoform-specific transcriptional activation, and suggested that a major aspect of receptor function could be explained at the most fundamental protein-DNA level. Nonetheless, receptor−promoter interactions still must be accompanied by coactivator recruitment in order to activate transcription. Thus we have investigated the mechanisms of promoter-dependent coactivator recruitment using the full-length PR-A isoform, the nuclear receptor interaction domain of SRC2, and promoters containing either one or two palindromic progesterone response elements (PREs).

Using quantitative footprinting and statistical thermodynamic modeling, we have resolved the microscopic energetic contributions to promoter-dependent coactivator binding. We find that the most significant linkage between receptor−promoter assembly and coactivator recruitment is not at the level of individual response elements, but rather is localized to cooperative interactions between response elements. This result may offer a framework for understanding why isolated response elements show little to no transcriptional activation ability, and why multisite promoters typically show strong activity that is synergistic in behavior (*10*). Because this nonadditive response arises due to coupling between coactivator recruitment and cooperative interactions between bound receptors, the results also suggest that coactivator levels *in vivo* could act as a physiological regulator of receptor−promoter stability.

EXPERIMENTAL PROCEDURES

Expression and Purification of the Human Progesterone Receptor A-Isoform and the Interaction Domain of SRC2. An expression vector encoding the full-length PR-A isoform (amino acids 165− 933 as diagramed in Figure 1A) fused to an N-terminal hexahistidine tag was a generous gift of Dr. Dean Edwards (Baylor College of Medicine). The receptor was expressed in baculovirus-infected Sf9 insect cells as previously described (*17*). A detailed description of the PR-A purification process and a quantitative analysis of its hydrodynamic and thermodynamic solution properties has been published previously (*18*). Briefly summarized, a global analysis of sedimentation velocity datasets collected at multiple PR-A concentrations demonstrated the presence of a hydrodynamically homogeneous 3.50 s monomer species in rapid equilibrium with a 7.15 s dimer species. Sedimentation equilibrium analysis under identical conditions demonstrated that self-association could be rigorously described using a monomer−dimer assembly reaction scheme with a dimerization free energy of -7.6 ± 0.6 kcal/mol.

A bacterial expression vector encoding residues 563−767 of mouse SRC2 fused to an N-terminal GST tag and C-terminal hexahistidine tag was a generous gift of Dr. Keith Yamamoto (University of California at San Francisco). The fusion protein was expressed in BL21 *Escherichia coli* cells grown at 37 °C. Cultures were allowed to grow to 0.7 OD

and then induced for 3−4 h using 1 mM IPTG. The cells were harvested by centrifugation, and all subsequent steps were performed at 4 °C. Pelleted cells were resuspended in 20 mM Tris pH 8.0, 150 mM NaCl, 5 mM EDTA, 5% w/v glycerol, and 2 mM β-mercaptoethanol. The resuspension was then sonicated, and cell debris was removed by centrifugation. The supernatant was incubated with Glutathione Sepharose 4B resin (GE Healthcare) in batch. The resin was washed extensively with the above lysis buffer, and then exchanged into an otherwise identical buffer containing 50 mM NaCl. The resin-bound protein was incubated overnight with 7U thrombin per mL bed-volume resin. The eluate from the cleavage reaction was directly loaded onto a Q Sepharose ion-exchange column (GE Healthcare) in order to remove thrombin and any remaining impurities. SRC2 was collected as a flow-through (due to it being the only protein that did not interact with the resin under these conditions) and flash-frozen. Coactivator concentration was determined using a calculated extinction coefficient of 2,680 M^{-1} cm^{-1} (*19*). Typical yields were 10−12 mg of SRC2 per liter of cell culture.

Sedimentation Velocity. Sedimentation was carried out on a Beckman XL-A analytical ultracentrifuge equipped with absorbance optics. A two channel Epon centerpiece and an An-60 Ti rotor were used. SRC2 was loaded at an initial concentration of 2 μM and sedimented at 4 °C in a buffer containing 20 mM Hepes, pH 8.0, 50 mM NaCl, 2.5 mM $MgCl_2$, 1 mM $CaCl_2$, 1 mM DTT, and 10^{-5} M progesterone. The protein was sedimented at a rotor speed of 50,000 rpm, with data collected at 230 nm and as quickly as the instrument would allow (typically every 4 min). In order to determine the $s_{20,w}$ and apparent molecular weights for species in solution (e.g., monomer), the data were fit directly to the Lamm equation as implemented in the program Sedfit (*20*) in order to determine the $c(s)$ and $c(M)$ distributions, respectively. The frictional coefficient (f) of the sedimenting species was determined using its resolved $s_{20,w}$ and the Svedberg equation:

$$s_{20,w} = M(1 - \bar{\nu}\rho)/Nf \quad (1)$$

where M is the molecular weight as calculated by the amino acid sequence and assembly stoichiometry, $\bar{\nu}$ is the partial specific volume of the protein, ρ is the water density at 20 °C, and N is Avogadro's number. The partial specific volume for SRC2 was calculated by summing up the partial specific volumes of each individual amino acid (0.7232 mL/g) (*21*). In order to calculate a frictional ratio (f/f_0), the frictional coefficient of a compact sphere of the same molecular weight (f_0) was calculated assuming a degree of hydration of 0.3 g of water/g of protein (*22*, *23*).

In order to assess the affect of SRC2 on PR-A solution assembly energetics, the receptor was subjected to sedimentation velocity analysis as a function of increasing SRC2 concentrations. Briefly, PR-A was sedimented at 1 μM concentration with 0.3, 1.0, or 7.0 μM SRC2 present. Solution conditions were identical to the SRC2 sedimentation velocity studies, except that the NaCl concentration was 300 mM due to the insolubility of PR-A at 1 μM concentration or greater when in low salt conditions. Data were analyzed using the program Sedfit (*20*) to determine the $c(s)$ distribution.

DNA Preparation for DNase I Footprinting. A vector containing a synthetic promoter made up of two tandemly linked PREs (PRE_2) was a generous gift of Dr. Kathryn Horwitz (University of Colorado Health Sciences Center). Each PRE corresponds to the palindromic tyrosine aminotransferase promoter sequence, TGTACAGGATGTTCT (*24*). The two PREs are spaced 25 base pairs apart and upstream of a thymidine kinase regulatory element. A reduced-valency template (PRE_{1-}) containing a G-to-T point mutation in each half-site of the distal PRE (designated as site 1) was created "in house". This point mutation eliminated receptor binding to site 1 (*16*, *25*). Each template was excised from its respective vector to generate a 1304 bp promoter fragment. The fragments were ^{32}P-end-labeled on the sense-strand using a Klenow fill-in reaction. The proximal PRE of each fragment (designated as site 2) was positioned 100 bp from the 3′ end of the labeled strand.

Individual-Site Binding Experiments. Experiments were carried out using quantitative DNase I footprint titrations as originally presented by Ackers and co-workers (*26*, *27*), and with modifications described previously (*15*, *16*). Briefly, all reactions were carried out in 20 mM Hepes, pH 8.0, 50 mM NaCl, 2.5 mM $MgCl_2$, 1 mM $CaCl_2$, 1 mM DTT, 10^{-5} M progesterone, 100 μg/mL BSA, and 2 μg/mL salmon sperm DNA at 4 °C. Each reaction contained 20,000 cpm of freshly labeled DNA containing either the PRE_2 or PRE_{1-} promoter. PR-A was added to each reaction sample, covering a concentration range from subnanomolar to micromolar either in the presence (at least 1μM) or in the absence of SRC2. Samples were allowed to equilibrate for at least 45 min. Upon reaching equilibrium, each sample was exposed to DNase I for exactly 2 min. Each reaction was then quenched, and the DNA products were electrophoresed on a 6% polyacrylamide−urea gel. The footprint titrations were visualized using phosphorimaging. Individual-site binding curves were calculated as described by Brenowitz et al. (*26*) using the program ImageQuant. All studies were carried out using DNase I concentrations that approximated "single hit" kinetics. Promoter DNA concentrations were estimated to be well below the PR-A intrinsic binding affinity, thus justifying the assumption that $PR\text{-}A_{free} \sim PR\text{-}A_{total}$.

Resolution of Microscopic Interaction Free Energies. The DNase I footprint titration technique resolves the fractional occupancy of binding at each PRE. The statistical thermodynamic expressions that describe the individual-site binding isotherms are constructed by summing the probabilities of each microscopic configuration that contributes to binding at that site. A detailed approach for generating each mathematical formulation has been presented previously (*28*). Briefly, the probability (f_s) of any microscopic configuration is defined as (*29*)

$$f_s = \frac{e^{-\Delta G_s/RT}[x]^j}{\sum_{s=1}^{j} e^{-\Delta G_s/RT}[x]^j} \quad (2)$$

where ΔG_s is the free energy of configuration state s relative to the unliganded reference state, x is the PR-A monomer concentration (as calculated from the dimerization constant, k_{di}), and j is the stoichiometry of PR-A monomer bound to a response element. R is the gas constant, and T is

temperature in kelvins. The relationship between each free energy change and its association constant is defined via the standard relationship $\Delta G_i = -RT \ln k_i$. Thus, the fractional saturation ($\bar{Y}$) for dimer binding at site 1 of the PRE_2 promoter is the sum of probabilities for the isolated dimer binding reaction and the cooperative binding reaction with the adjacently bound dimer. When the equation for PR-A dimer binding to site 1 on the PRE_2 is expressed in terms of free PR-A monomer concentration, the fractional saturation is then defined as

$$\bar{Y}_{PRE_2} = \frac{k_{di}k_2x^2 + k_{di}^2k_2^2k_{c2}x^4}{1 + 2k_{di}k_2x^2 + k_{di}^2k_2^2k_{c2}x^4} \quad (3)$$

where k_{di} and x are as defined previously, k_2 is the intrinsic association constant for a preformed dimer binding to a PRE, and k_{c2} corresponds to the intersite cooperativity term. Because the PREs are identical in sequence, eq 2 also describes binding to site 2 of the PRE_2 promoter. Using the same approach, the equation describing the fractional saturation of site 2 of the PRE_{1-} promoter is

$$\bar{Y}_{PRE_{1-}} = \frac{k_{di}k_2x^2}{1 + k_{di}k_2x^2} \quad (4)$$

The equations describing a pathway by which successive monomers bind to the PRE_2 and the PRE_{1-} promoters are generated using a similar approach and have been presented previously (*16*). However, in this case the relevant parameters are k_1, the intrinsic affinity of monomer binding; k_{c1}, the intrasite cooperativity; and k_{c2}, the intersite cooperativity. As discussed later in the text, the previously determined PR-A dimerization constant, k_{di}, was assumed to be unaffected by the presence SRC2.

In order to resolve each set of interaction parameters that describe PR-A:DNA binding, the individual-site binding isotherms from each footprint titration were analyzed simultaneously using the program Scientist (Micromath, Inc.). Because protein interactions at specific DNA binding sites do not afford complete protection from DNase activity, binding data were treated as transition curves ($\bar{Y}_{app}$) fitted to upper (m) and lower (b) endpoints using the equation

$$\bar{Y}_{app} = b + (m - b)\bar{Y} \quad (5)$$

RESULTS

Theoretical Approach. As diagramed in Figure 2A, the commonly accepted binding pathway for PR-promoter assembly is that hormone-bound receptors dimerize in solution and bind at palindromic response elements (*1*). The affinity of solution dimerization is defined as ΔG_{di}, and that of preformed dimer binding is defined as ΔG_2, the intrinsic binding free energy. For promoters containing tandemly linked response elements, binding is also coupled to cooperative interactions between each site, described by the term ΔG_{c2}. Also described is a thermodynamically equivalent monomer binding pathway (Figure 2B) in which PR-A monomers bind to individual half-sites with an affinity of ΔG_1 and an intrasite cooperativity of ΔG_{c1}. Intersite cooperativity between the sites is as described for the dimer binding pathway. It is important to note that apparent binding affinities as determined by gel-shift assays, for example, reflect an irreducible composite of the dimerization energetics and intrinsic binding energetics, and are thus of limited utility for the type of analyses described here.

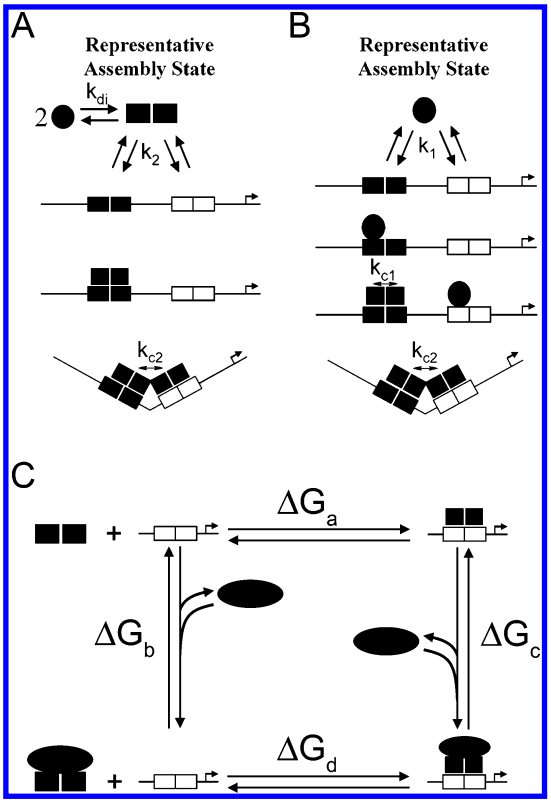

FIGURE 2: Schematic representation of selected assembly states for PR-A:PRE_2 interactions and thermodynamic cycle for SRC2 interactions. (A) Dimer binding pathway: Filled circles represent hormone-bound PR-A structure prior to either solution dimerization (k_{di}) or binding at a PRE (k_2). Filled squares represent PR-A solution dimers or PR-A bound to the PRE_2 promoter template. Only preformed PR-A dimers are competent to assemble at palindromic response elements. Binding at multiple response elements is accompanied by cooperative interactions between the sites (k_{c2}; defined here as "intersite cooperativity") seen as direct contact of adjacently bound dimers and induction of DNA bending. (B) Monomer binding pathway: PR-A assembles at palindromic response elements via a succession of monomer-binding reactions (k_1). Successive binding at an individual response element is accompanied by cooperative interactions (k_{c1}; defined here as "intrasite cooperativity") and represented by a transition from a filled circle to a filled square. In both panels, PRE binding sites within the PRE_2 template are represented by a solid rectangle (site 1) and open rectangle (site 2). Separating each half site within each PRE is a white line (site 1) or a black line (site 2). Arrow refers to the direction of transcriptional start site. (C) Thermodynamic cycle representing SRC2 recruitment to the promoter. SRC2 can follow a pathway of either binding to a preformed PR-A dimer:promoter complex ($\Delta G_a + \Delta G_c$) or interacting with unbound PR-A dimer prior to promoter binding ($\Delta G_b + \Delta G_d$). Equilibrium constants are related to the free energy changes through the standard expression $\Delta G_i = -RT \ln k_i$.

In order to effect transcriptional activation, receptor−promoter interactions are also coupled to enhanced coactivator interactions (i.e., "recruitment") through an allosteric linkage mechanism (Figure 2C). The extent of this linkage ($\Delta\Delta G_{recruit}$) can be quantitated as the difference in binding affinity between coactivator:PR-A assembly in the presence (ΔG_c) and absence (ΔG_b) of DNA:

$$\Delta\Delta G_{recruit} = \Delta G_c - \Delta G_b \quad (6)$$

Unfortunately, as defined, this parameter is not easily measured experimentally. However, since the schematic in Figure 2C represents a thermodynamic cycle, it is equally valid to define the energetics of recruitment as the difference in binding affinities between PR-A:DNA assembly in the presence (ΔG_d) and absence (ΔG_a) of coactivator:

$$\Delta\Delta G_{recruit} = \Delta G_d - \Delta G_a = \Delta G_c - \Delta G_b \qquad (7)$$

This latter definition is experimentally accessible simply by determining the binding affinities of PR-A:DNA interactions in the absence of coactivator and presence of coactivator. Under conditions in which coactivator is saturating at the promoter, the free energy change represents the total amount of energy necessary for recruitment. And as we describe in more detail below, this approach can be expanded in order to localize the origins of recruitment to the various microstate interactions that define assembly at more complex, multisite promoters. However, in order to ensure that the resolved energetics actually represent physically meaningful values, it is necessary to first demonstrate that all components are structurally and functionally homogeneous. We previously characterized PR-A self-assembly energetics using analytical ultracentrifugation and cooperative PR-A:promoter energetics using quantitative footprint titrations (*15*, *18*); here we use a similar approach to first analyze the solution properties of SRC2 and then resolve the energetics of SRC2 recruitment to promoters containing individual and multiple response elements.

The SRC2 Interaction Domain Exists as a Homogeneous, but Structurally Asymmetric, Monomer. Milligram quantities of the interaction domain of mouse SRC2 (Figure 1B) were purified from BL21 *E. coli* cells as described in Experimental Procedures. SDS−PAGE analysis showed that SRC2 was at least 98% pure as judged by densitometric analysis of Coomassie Blue-stained gels (data not shown). Sedimentation velocity analysis was used to examine the hydrodynamic properties of SRC2 under concentrations and conditions identical to those used in the subsequent footprinting studies. Shown in Figure 3 are the results of a *c*(*M*) analysis (*20*) of the velocity data. Direct fitting of the raw data using Sedfit resolved a peak molecular mass of 21,209 kDa, in close agreement with the calculated monomer mass of 21,782, thus demonstrating that SRC2 is quantitatively monomeric under these conditions. Using the Svedberg equation (eq 1) and the monomer molecular mass, we calculate a frictional coefficient (*f*) of 6.84×10^{-8} g/s. Comparison of the frictional coefficient to that of a hydrated sphere of identical mass (f_o) indicates that SRC2 is highly asymmetric with a frictional ratio (f/f_o) of 2.1. Modeling of SRC2 as a hydrated prolate ellipsoid yields a ratio of major to minor axes of 20:1 and a Stokes radius of 35 Å. CD spectrometry and limited proteolysis of SRC2 indicate that the significant asymmetry of SRC2 is due to a largely disordered structure (data not shown), consistent with other analyses of coactivator structure (*30*).

SRC2 Interacts Only Weakly with PR-A in the Absence of DNA. As described in Experimental Procedures, an assumption of the statistical thermodynamic analysis is that SRC2 does not significantly perturb PR-A solution assembly energetics. As an explicit test of this assumption, we analyzed PR-A:SRC2 interactions in the absence of DNA using

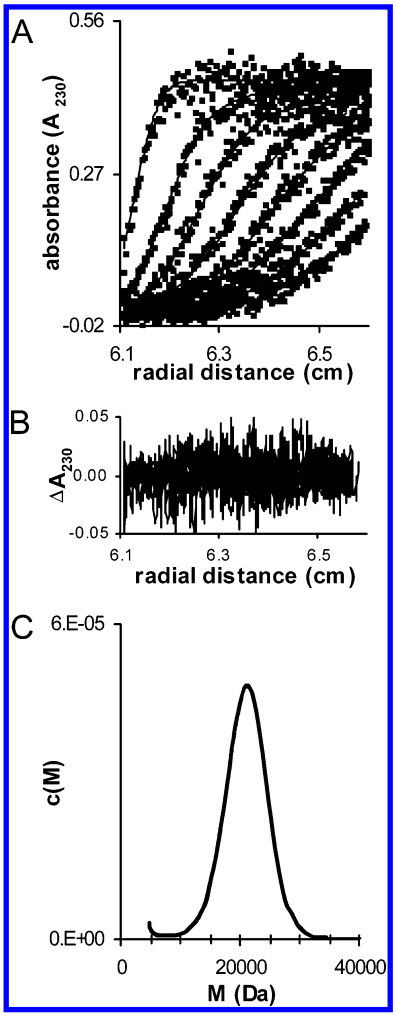

FIGURE 3: Sedfit analysis of SRC2 at pH 8.0, 50 mM NaCl, and 4 °C. (A) Initial protein loading concentration was 2.0 μM. Every fourth scan for SRC2 at 50,000 rpm is plotted as a function of radial position. Solid lines represent an analysis to these data using the *c*(*M*) model from Sedfit. (B) The residuals of the fit from the *c*(*M*) analysis. (C) The *c*(*M*) distribution resolves a most probable molecular mass peak corresponding to 21,209 Da in close agreement with the calculated molecular weight of 21,782 Da.

sedimentation velocity. Shown in Figure 4 are the results of a *c*(*s*) analysis of PR-A sedimentation as a function of increasing SRC2 concentration. At 1 μM concentration of PR-A, the receptor exists as both monomers and dimers in rapid equilibrium (*18*). This distribution is reflected as the single sedimentation coefficient distribution peaked at approximately 3.9 S. Introduction of approximately equimolar concentrations of coactivator results in a free SRC2 distribution at 1.5 S and the weak appearance of higher order sedimenting species ranging from 6 S up to 25 S. Increasing concentrations of SRC2 resulted in increased presence of the higher order products, but only mildly shifted the distribution of the PR-A monomer−dimer peak. The peaks observed at larger *s* values are seen only when PR-A and SRC2 are allowed to interact, and thus demonstrate that coactivator induces formation of higher-order assembly complexes. However, their low population relative to free SRC2 and PR-A indicates that receptor−coactivator interactions are energetically weak under these solution conditions.

The sedimentation results are in qualitative agreement with earlier biochemical studies that indicated that SRC2−thyroid receptor interactions were of apparent micromolar affinity

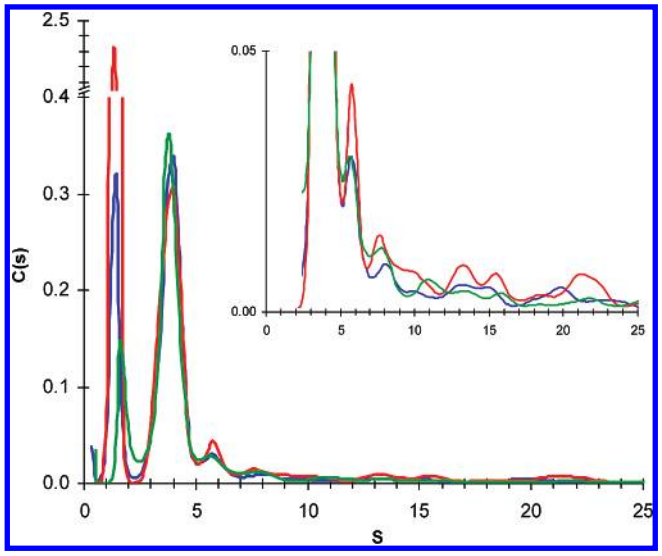

FIGURE 4: *c*(*s*) analysis of PR-A and SRC2 complex at pH 8.0, 300 mM NaCl, 4 °C. Initial protein loading concentration for PR-A was 1.0 μM for all three samples. Initial protein loading concentrations for SRC2 were 0.3 μM (green), 1 μM (blue), and 7 μM (red). A continuous size distribution, *c*(*s*), was calculated using the program Sedfit. Inset shows the *c*(*s*) distribution at higher resolution in order to emphasize the appearance of faster sedimenting species. For clarity, only data from 2 to 25 s are shown.

(*13*), and also demonstrate that SRC does not significantly perturb PR-A assembly energetics under these conditions. However, as noted in Experimental Procedures, these studies were necessarily carried out at 300 mM NaCl, whereas our footprint titrations were carried out at 50 mM NaCl. Due to experimental complexity, it is not possible to easily measure the energetics of SRC2:PR-A interactions at low salt concentrations. However, our previously published results demonstrate that PR-A self-association is independent of NaCl concentrations ranging from 50 mM to 1 M (*15*, *18*). Furthermore, computer simulations demonstrate that the resolved DNA binding energetics are statistically unchanged when the PR-A dimerization affinity is varied by as much as 40-fold (data not shown). Thus for the purposes of analysis, we assume that SRC2 does not significantly perturb PR-A dimerization energetics at 50 mM NaCl.

SRC2 Modulates PR-A Intrinsic and Cooperative DNA Binding Energetics. Shown in Figure 5A is a quantitative footprint titration of the PRE_2 promoter template. The template was titrated with increasing concentrations of PR-A in the presence of 1 μM SRC2. (The resolved binding isotherms were found to be identical once in the presence of 1 μM or greater SRC2, indicating that the coactivator was at saturating concentrations with regard to DNA binding.) It is evident that PR-A binds to each PRE with a high degree of specificity: Dideoxy sequencing analysis indicates that site-specific binding results in the protection of each palindromic PRE and approximately one to two flanking nucleotides. These interactions are coupled to the appearance of hypersensitive sites adjacent to each PRE and centrally located between the PREs (arrows). We have previously interpreted these sites as being reflective of PR induced DNA bending and promoter distortion (*15*, *16*); however, the extent of hypersensitivity does not change as a function of SRC2 concentration indicating that it does not play a role in this phenomenon.

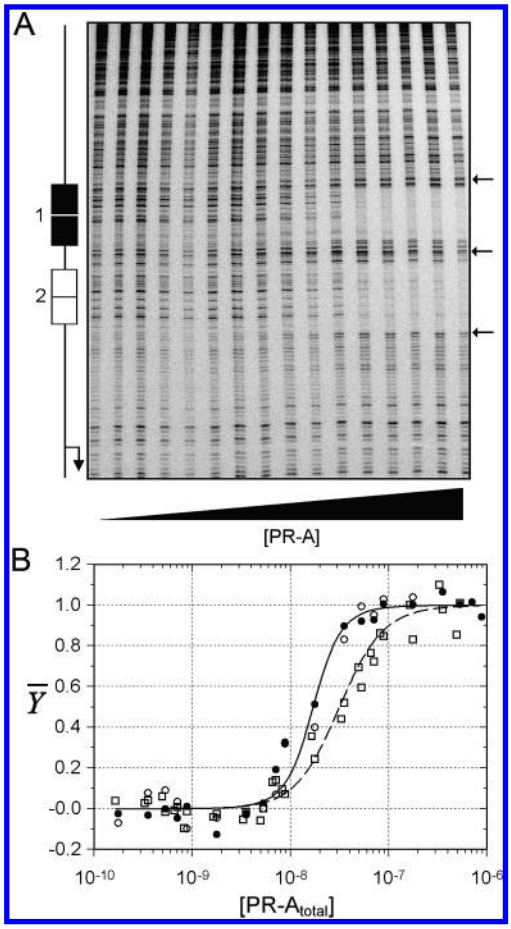

FIGURE 5: Representative quantitative footprint titration and individual-site binding isotherms obtained for PR-A assembly at the PRE_2 promoter in the presence of saturating concentration of SRC2. (A) PRE_2 footprint titration image. Schematic of PRE_2 promoter structure is shown to left. Arrows right of image indicate the appearance of hypersensitive bands. (B) PR-A binding isotherms for assembly at site 1 (filled circles) and site 2 (open circles) of the PRE_2 promoter and assembly at site 2 (open squares) of the PRE_{1-} promoter. The lines through the data represent best-fit global analysis of six datasets to the dimer binding pathway model as described in Experimental Procedures. For clarity, only a representative subset of data is shown. The monomer binding pathway model generated identical results and is thus not shown.

Shown in Figure 5B is a set of representative individual site binding isotherms for PR-A binding to the PRE_2 promoter and to a PRE_{1-} promoter lacking a functional site 2. When plotted in units of total PR-A concentration, it is evident that half-saturation of an isolated PRE occurs at approximately 30 nM. By contrast, addition of a second site changes the apparent affinity to 16 nM, indicative of cooperative interactions between sites. However, because these data sets are presented in units of total protein concentration rather than in units of a presumed binding species (e.g., dimer) as determined by the dimerization constant, the half-saturation values have little mechanistic value. In order to determine physically meaningful interaction constants, we globally fit the datasets to a model in which preformed PR-A dimers could bind to the PREs and undergo cooperative interactions between PREs (Figure 2A and eqs 3−5). The analysis resolves the intrinsic and cooperative binding energetics associated with PR-A:DNA binding. Since we are not specifically analyzing the energetics of SRC2 binding interactions with PR-A (ΔG_b or ΔG_c as defined in

Table 1: Resolved Energetics for PR-A:Promoter Binding in the Presence and Absence of SRC2

interaction free energy	(+)SRC2, kcal/mol	(−)SRC2, kcal/mol
ΔG_1	-8.7 ± 0.2	-8.3 ± 0.3
ΔG_{c1}	-1.4 ± 0.5	-2.1 ± 0.8
ΔG_{c2}	-1.9 ± 0.3	-0.6 ± 0.2
ΔG_2	-11.7 ± 0.1	-11.4 ± 0.1
ΔG_{c2}	-1.3 ± 0.2	-0.4 ± 0.2
ΔG_{di}	-7.6 ± 0.6	-7.6 ± 0.6

Table 2: Energetic Differences for PR-A:Promoter Binding in the Presence and Absence of SRC2[a]

interaction free energy	$\Delta\Delta G$, kcal/mol
ΔG_1	-0.4 ± 0.4
ΔG_{c1}	0.7 ± 0.9
ΔG_{c2}	-1.3 ± 0.4
ΔG_2	-0.3 ± 0.1
ΔG_{c2}	-0.9 ± 0.3
ΔG_{di}	

[a] Errors propagated from Table 1 using standard procedures (*40*).

Figure 2C), but only the change in PR-A energetics in the presence of SRC2 ($\Delta\Delta G_i$), it is unnecessary to explicitly add an SRC2 binding parameter to the mathematical model.

As noted by the lines in Figure 5B, the model does an excellent job in describing the apparent affinities, curve shapes, and increased cooperative contributions for PR-A binding. The resolved interaction energetics are presented in Table 1. As shown, the intrinsic energetics of preformed dimer binding to a PRE is −11.7 kcal/mol. This value translates to a dissociation constant of 0.6 nM at 4 °C. The discrepancy between the resolved constant and the apparent value is simply because the data are plotted in units of total protein concentration rather than in dimer concentration (as determined by the independently determined dimerization constant). For the same reason, the intersite cooperativity, determined to be −1.3 kcal/mol or an over 10-fold increase, is seen as only a 2-fold effect. Finally, since the binding curves reflect binding at individual sites rather than the overall, macroscopic binding reaction, the contribution of cooperative energetics to each curve is partitioned as the square root of the approximately 10-fold increase (*31*).

Based on our previous work demonstrating that PR self-associates only in the micromolar range under conditions in which the DNA binding affinity is in the nanomolar range, we also fit the data to a monomer pathway binding model, which assumes that a dimeric receptor−DNA complex only occurs through successive monomer binding and a DNA-induced dimerization reaction. Analysis of the data using this model resolves a monomer intrinsic affinity of −8.7 kcal/mol, an intrasite cooperativity of −1.4 kcal/mol, and an intersite cooperativity of −1.9 kcal/mol. Importantly, the monomer and dimer binding pathway models are thermodynamically identical as evidenced by their equivalence in saturating the PRE_2 promoter: The total energy of assembly by the monomer pathway model is -39.5 ± 1.3 kcal/mol, whereas by the dimer pathway free energy it is -39.9 ± 1.2 kcal/mol. We note, however, that the slight difference of 0.4 kcal/mol in the total energy of assembly is seen in both the presence and absence of SRC2. This small discrepancy may suggest that there are secondary levels of cooperativity not accounted for in our models (e.g., an intersite cooperative interaction occurring in the triply ligated state of the monomer binding pathway.) We are currently investigating this possibility through the use of additional reduced valency templates.

Shown in Table 2 are the differences in PR-A:DNA binding energetics, in the presence and absence of SRC2, as determined by matched experiments carried out under identical solution conditions. First, it is worth noting that the free energy changes for PR-A:PRE_2 binding in the absence of SRC2 are statistically identical to our previously published studies (*15*), thus demonstrating the precision of the experimental approach. Second, the differences in energetics as a function of coactivator reveal only a modest −0.3 kcal/mol increase in dimer intrinsic binding affinity, translating to only a 2-fold effect. Likewise cooperative monomer assembly at the palindrome is increased by only −0.1 kcal/mol. By contrast, regardless of binding model, cooperative energetics are increased by −0.9 (dimer model) to −1.3 kcal/mol (monomer model), translating to an additional 6- to 10-fold increase in stability. These results thus localize the major energetic contribution of coactivator recruitment to cooperative interactions between palindromic binding sites.

DISCUSSION

We demonstrate here that PR-A binding to both individual and multiple response elements is enhanced in the presence of the coactivator, SRC2. As outlined earlier, any SRC2-dependent increase in receptor binding energetics ($\Delta\Delta G_i$) is equivalent to an increase in SRC2 affinity to the promoter-bound receptor. Therefore, the changes noted in Table 2 simultaneously reflect the energetics of receptor:promoter interactions as a function of coactivator, and receptor:coactivator interactions as a function of promoter. Importantly, these results are not an artifact of protein activity (via SRC2-dependent dissolution of receptor aggregates, for example) since we have rigorously demonstrated that both PR-A (*18*) and SRC2 (Figure 3) are structurally and functionally homogeneous under these conditions. Nor do the results arise from simply enriching a tetrameric PR-A assembly state, since statistically different increases in binding energetics are also observed for receptor dimer binding events. Finally, the observed phenomenon is unlikely to be due to artifacts from using a deletion construct since our analyses of full-length SRC3 coactivator generate similar results. Specifically, preliminary studies demonstrate that SRC3 enhances intersite cooperativity by -1.5 ± 0.4 kcal/mol, in close agreement with the results seen in Table 2 (A.F.H. and D.L.B., manuscript in preparation).

Synergistic Recruitment of SRC2. As seen in Table 2, assembly of a PR-A dimer at a palindromic PRE is maximally coupled to a −0.1 to −0.3 kcal/mol enhancement in SRC2 binding affinity, depending on the binding pathway. Furthermore, PR-A binding to a promoter containing two PREs is coupled to an additional −0.9 to −1.3 kcal/mol increase in stability. Since SRC2 presumably does not directly interact with DNA, the resolved energetics quantitatively reveal PR-A as a mediator of heterotropic allostery. From a functional perspective, the results may offer a molecular explanation for the negligible transcriptional

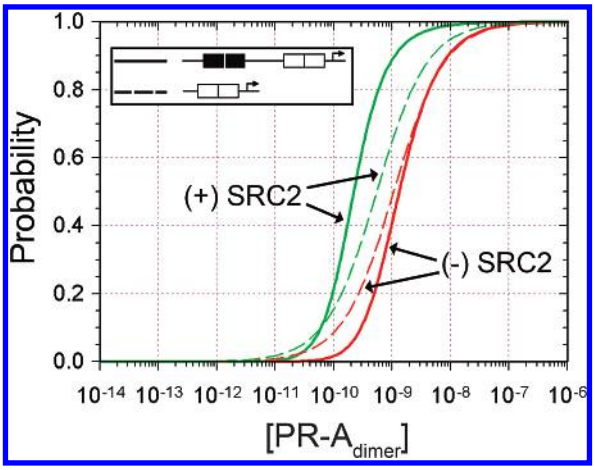

FIGURE 6: Calculated probabilities of the PR-A dependent, fully ligated PRE_2 and PRE_{1-} promoters in the presence and absence of SRC2. Solid line (red) represents the fully saturated PRE_2 promoter in the absence of SRC2. Dashed line (red) represents the fully saturated PRE_{1-} promoter in the absence of SRC2. Solid line (green) represents the fully saturated PRE_2 promoter in the presence of SRC2. Dashed line (green) represents the fully saturated PRE_{1-} promoter in the presence of SRC2. Probabilities were calculated based on the experimentally determined interaction energetics presented in Table 1.

activity observed for promoters containing a single response element and the synergistic, nonadditive increase in activity seen when a promoter contains multiple response elements (*10*).

As an illustration of the above argument, shown in Figure 6 is the calculated probability of observing the fully ligated PR-A:PRE_2 microstate (the presumptive transcriptionally active microspecies) as determined from the resolved energetics, compared to the predicted probability of the fully ligated PRE_{1-} promoter. Also shown are the respective probabilities in the presence of SRC2. In order to better clarify the relationship between the energetics and promoter occupancy by PR-A, the data is presented in units of a model-dependent active binding species (free PR-A dimer concentration), as calculated from the dimerization constant and conservation of mass equation. Under the condition in which no coactivator is present, it is evident that the probability of observing either fully ligated promoter is nearly identical, particularly at values greater than 0.5. However, the presence of saturating amounts of SRC2 generates a considerable difference in the probabilities for the two promoter configurations. In particular, the PRE_{1-} probability is only mildly influenced by SRC2 as now properly noted by the subtle 2-fold change in the apparent half-saturation value. By contrast, the apparent affinity for the fully ligated PRE_2 promoter is greatly increased as predicted by the dimer pathway energetics in Table 2. Perhaps more importantly, it is clear that, regardless of PR-A dimer concentration, the presence of SRC2 generates only an incremental increase in the probability of observing a PR-A bound PRE_{1-} promoter. However, SRC2 significantly enhances the probability of observing the fully ligated PRE_2 promoter in the physiologically relevant concentration range of 10^{-10} to 10^{-8} molar. These observations thus suggest that it is the linkage between cooperative receptor binding and coactivator recruitment, rather than simply DNA binding and coactivator recruitment, that explains the synergistic transcriptional response often observed between receptor-regulated promoters containing either one or two PRE binding sites (*10*).

Given these results, why is PR-A traditionally thought of as a weak transcriptional activator? This interpretation is in part due to the poor ability of PR-A to activate reporter genes containing a single upstream PRE, and only modestly activate genes containing two PREs (i.e., the synthetic PRE_2 promoter described here) (*4*). Additionally, the PR-A counterpart, PR-B, is a much stronger transactivator on the PRE_2 template (yet still transcriptionally weak on a promoter containing a single PRE (*4*)). However, recent microarray studies have demonstrated that PR-B and PR-A are both capable of acting as either strong or weak transcriptional activators depending upon the particular promoter sequence (*9*). These observations thus raise a question about the fundamental origins of isoform-specific functional differences. Biochemical studies have suggested that a key difference in isoform-specific transcriptional activity is due to differential interactions with coactivators such as SRC2 (*32*). Specifically, pull-down assays and transient transfection studies indicated that the transcriptionally stronger B-isoform could preferentially interact with the coactivator, SRC2, whereas PR-A only weakly interacted with SRC2, but more strongly interacted with the corepressor, SMRT. However, our work here unambiguously demonstrates that PR-A is perfectly capable of recruiting coactivators, and can do so when bound to multiple promoter types. Furthermore, rigorous, thermodynamic analysis of PR-A and PR-B promoter interactions suggests that a major aspect of isoform-specific functional differences arises not from differential recruitment but from differences in cooperative binding energetics (*15*).

In this light, the weak transcriptional activity seen for PR-A when bound to an isolated response element (e.g., PRE_{1-}) is likely due to a combination of decreased DNA binding affinity and modest coactivator recruitment energetics. However, since PR-A can greatly increase SRC2 recruitment to a PRE_2 promoter via enhanced cooperative interactions, its continued weak activity on this promoter *in vivo* may be due to limiting cellular concentrations of coactivator. Consistent with this are studies demonstrating that overexpression of SRC2 has little effect on PR-A activity at a single PRE, but generates a 4-fold synergistic effect on a PRE_2 promoter (H. Abdel-Hafiz and K. B. Horwitz, personal communication.) Whether the B-isoform follows a similar profile in its ability to recruit coactivators is currently under investigation.

What Is the Structural Basis of PR-A:SRC2 Recruitment? Nuclear receptor−coactivator interactions are often considered within the stereochemical framework of an LXXLL coactivator helix interacting with a hydrophobic pocket within the receptor LBD (*33*). The observed ability of DNA to influence this interaction suggests that there is allosteric communication between the DBD and the LBD. In the context of a single PRE, classical models would suggest that DNA-bound dimers generate quaternary-level structural changes that trigger high affinity SRC2 binding. Consistent with this are biochemical and biophysical data indicating that PR structure is indeed modulated as a function of DNA binding (*34*, *35*). How SRC2 might stabilize intersite cooperative interactions is less clear. If PR-A cooperativity is mediated by direct protein−protein interactions, then it is likely that enhanced recruitment results from preferential

coactivator interactions with higher-order receptor complexes. This interpretation may lend insight into the appearance of faster sedimenting species seen in our PR-A:SRC2 sedimentation velocity analysis (Figure 4).

SRC2 as a Regulator of Cooperative PR-A Assembly. The commonly accepted framework for interpreting nuclear receptor transcriptional regulation is that, upon binding promoter sequences, the proteins trigger coactivator recruitment via enhanced receptor−coactivator binding affinities. If, however, these reactions are occurring via allosteric mechanisms, then it thermodynamically must be the case that coactivators modulate receptor−DNA binding affinities. In the case of PR-A interactions at the PRE_2 promoter, the basis for this phenomenon localizes to enhanced cooperative binding energetics between adjacently bound receptor dimers. In other words, increased SRC2 concentrations stabilize a higher-order PR-A assembly complex. This linkage relationship is perhaps not surprising, since physiologically regulated cooperative assembly is a phenomenon seen for many transcription factors (*36*, *37*). Generally, cooperativity serves as a means to generate a highly efficient molecular switch: Only small changes in ligand levels translate into major changes in macromolecular occupancy relative to a noncooperative system. However, the functional purpose of cooperativity is specific to each interacting system. For example, cooperativity in the classical λ repressor-right operator system exists to stabilize the lysogenic state as well as carry out an efficient transition to the lytic phase (*28*, *38*). By contrast, it may be that the physiological purpose of cooperative PR-A interactions is to recruit coactivators for transcriptional activation. This may explain why analysis of natural, nuclear receptor promoter sequences uniformly reveals the presence of multiple receptor binding sites but rarely a single, isolated binding site (*10*). Additionally, the linkage between coactivator binding and cooperative assembly implies that the receptor−promoter interactions, and thus functions, are "tunable" simply by regulating coactivator levels. Consistent with this notion is the observed correlation between overexpression of the coactivator, Amplified in Breast Cancer 1 (AIB1 or SRC3), and breast tumors (*39*). However, any meaningful test of these possibilities will first require a more mechanistic and predictive understanding of the roles that chromatin, nucleosomes, and the remodeling machinery play in regulating gene expression.

ACKNOWLEDGMENT

We thank Drs. Dean Edwards, Kathryn Horwitz, and Keith Yamamoto for constructs. We thank Amie Moody for helpful discussions and input.

REFERENCES

1. Tsai, M. J., and O'Malley, B. W. (1994) Molecular Mechanisms of Action of Steroid/Thyroid Receptor Superfamily Members, *Annu. Rev. Biochem. 63*, 451−486.
2. Lefstin, J. A., and Yamamoto, K. R. (1998) Allosteric Effects of DNA on Transcriptional Regulators, *Nature 392*, 885−888.
3. Meyer, M. E., Quirin-Stricker, C., Lerouge, T., Bocquel, M. T., and Gronemeyer, H. (1992) A Limiting Factor Mediates the Differential Activation of Promoters by the Human Progesterone Receptor Isoforms, *J. Biol. Chem. 267*, 10882−10887.
4. Sartorius, C. A., Melville, M. Y., Hovland, A. R., Tung, L., Takimoto, G. S., and Horwitz, K. B. (1994) A Third Transactivation Function (AF3) of Human Progesterone Receptors Located in the Unique N-Terminal Segement of the B-Isoform, *Mol. Endocrinol. 8*, 1347−1360.
5. Hopp, T. A., Weiss, H. L., Hilsenbeck, S. G., Cui, Y., Alfred, D. C., Horwitz, K. B., and Fuqua, S. A. (2004) Breast Cancer Patients with Progesterone Receptor PR-A-Rich Tumors Have Poorer Disease-Free Survival Rates, *Clin. Cancer Res. 15*, 2751−2760.
6. Meyer, M. E., Pornon, A., Ji, J. W., Bocquel, M. T., Chambon, P., and Gronemeyer, H. (1990) Agonistic and Antagonistic Activities of RU486 on the Functions of the Human Progesterone Receptor, *The EMBO J. 9*, 3923−3932.
7. Mulac-Jericevic, B., Lydon, J. P., DeMayo, F. J., and Conneely, O. M. (2003) Defective Mammary Gland Morphogenesis in Mice Lacking the Progesterone Receptor B Isoform, *Proc. Natl. Acad. Sci. U.S.A. 100*, 9744−9749.
8. Mulac-Jericevic, B., Mullinax, R. A., DeMayo, F. J., Lydon, J. P., and Conneely, O. M. (2000) Subgroup of Reproductive Functions of Progesterone Mediated by Progesterone Receptor-B Isoform, *Science 289*, 1751−1754.
9. Richer, J. K., Jacobsen, B. M., Manning, N. G., Abel, M. G., Wolf, D. M., and Horwitz, K. B. (2002) Differential Gene Regulation by the Two Progesterone Receptor Isoforms in Human Breast Cancer Cells, *J. Biol. Chem. 277*, 5209−5218.
10. Tung, L., Abdel-Hafiz, H., Shen, T., Harvell, D. M. E., Nitao, L. K., Richer, J. K., Sartorius, C. A., Takimoto, G. S., and Horwitz, K. B. (2006) Progesterone Receptors (PR)-B and -A Regulate Transcription by Different Mechanisms: AF-3 Exerts Regulatory Control over Coactivator Binding to PR-B, *Mol. Endocrinol. 20*, 2656−2670.
11. Xu, J., and Li, Q. (2003) Review of the In Vivo Functions of the P160 Steroid Receptor Coactivator Family, *Mol. Endocrinol. 17*, 1681−1692.
12. Hong, H., Kohli, K., Trivedi, A., Johnson, D. L., and Stallcup, M. R. (1996) GRIP1, a Novel Mouse Protein That Serves as a Transcriptional Coactivator in Yeast for the Hormone Binding Domains of Steroid Receptors, *Proc. Natl. Acad. Sci. U.S.A. 93*, 4948−4952.
13. Darimont, B. D., Wagner, R. L., Apriletti, J. W., Stallcup, M. R., Kushner, P. J., Baxter, J. D., Fletterick, R. J., and Yamamoto, K. R. (1998) Structure and Specificity of Nuclear Receptor-Coactivator Interactions, *Genes Dev. 12*, 3343−3356.
14. Li, X., Wong, J., Tsai, S. Y., Tsai, M.-J., and O'Malley, B. W. (2003) Progesterone and Glucocorticoid Receptors Recruit Distinct Coactivator Complexes and Promote Distinct Patterns of Local Chromatin Modification, *Mol. Cell. Biol. 23*, 3763−3773.
15. Connaghan-Jones, K. D., Heneghan, A. F., Miura, M. T., and Bain, D. L. (2007) Thermodynamic Analysis of Progesterone Receptor-Promoter Interactions Reveals a Molecular Model for Isoform-Specific Function, *Proc. Natl. Acad. Sci. U.S.A. 104*, 2187−2192.
16. Heneghan, A. F., Connaghan-Jones, K. D., Miura, M. T., and Bain, D. L. (2006) Cooperative DNA Binding by the B-Isoform of Human Progesterone Receptor: Thermodynamic Analysis Reveals Strongly Favorable and Unfavorable Contributions to Assembly, *Biochemistry 45*, 3285−3296.
17. Christensen, K., Estes, P. A., Onate, S. A., Beck, C. A., DeMarzo, A., Altmann, M., Lieberman, B. A., St John, J., Nordeen, S. K., and Edwards, D. P. (1991) Characterization and Functional Properties of the A and B Forms of Human Progesterone Receptors Synthesized in a Baculovirus System, *Mol. Endocrinol. 5*, 1755−1770.
18. Connaghan-Jones, K. D., Heneghan, A. F., Miura, M. T., and Bain, D. L. (2006) Hydrodynamic Analysis of the Human Progesterone Receptor A-Isoform Reveals that Self-Association Occurs in the Micromolar Range, *Biochemistry 45*, 12090−12099.
19. Gill, S., and von Hippel, P. (1989) Calculation of Protein Extinction Coefficients from Amino Acid Sequence Data, *Anal. Biochem. 182*, 319−326.
20. Schuck, P. (2003) On the Analysis of Protein Self-Association by Sedimentation Velocity Analytical Ultracentrifugation, *Anal. Biochem. 320*, 104−124.
21. Cohn, E. J., and Edsall, J. T. (1943) *Proteins, Amino Acids and Peptides*, Reinhold, New York.
22. Passen, H., and Kumosinski, T. F. (1985) Measurements of Protein Hydration by Various Techniques, *Methods Enzymol. 117*, 219−255.
23. Waxman, E., Laws, W. R., Laue, T. M., Nemerson, Y., and Ross, J. B. A. (1993) Human Factor VIIA and Its Complex with Soluble Tissue Factor: Evaluation of Symmetry and Conformational Dynamics by Ultracentrifugation and Fluoresence Anisotropy Decay Methods, *Biochemistry 32*, 3005−3012.

24. Jantzen, H. M., Strahle, U., Gloss, B., Stewart, F., Schmid, W., Boshart, M., Miksicek, R., and Schutz, G. (1987) Cooperativity of Glucocorticoid Response Elements Located Far Upstream of the Tyrosine Aminotransferase Gene, *Cell 49*, 29−38.
25. Eriksson, P., and Wrange, O. (1990) Protein-Protein Contacts in the Glucocorticoid Receptor Homodimer Influence Its DNA Binding Properties, *J. Biol. Chem. 265*, 3535−3542.
26. Brenowitz, M., Senear, D. F., Shea, M. A., and Ackers, G. K. (1986) Quantitative DNase Footprint Titration: A Method for Studying Protein-DNA Interactions, *Methods Enzymol. 130*, 132−181.
27. Brenowitz, M., Senear, D. F., Shea, M. A., and Ackers, G. K. (1986) Footprint Titrations Yield Valid Thermodynamic Isotherms, *Proc. Natl. Acad. Sci. U.S.A. 83*, 8462−8466.
28. Ackers, G. K., Johnson, A. D., and Shea, M. A. (1982) Quantitative Model for Gene Regulation by Lambda Phage Repressor, *Proc. Natl. Acad. Sci. U.S.A. 79*, 1129−1133.
29. Hill, T. L. (1960) *An Introduction to Statistical Thermodynamics*, Dover Publications.
30. Demarest, S. J., Martinez-Yamout, M., Chung, J., Chen, H., Xu, W., Dyson, H. J., Evans, R. M., and Wright, P. E. (2002) Mutual Synergistic Folding in Recruitment of CBP/p300 by p160 Nuclear Receptor Coactivators, *Nature 415*, 549−553.
31. Ackers, G. K., Shea, M. A., and Smith, F. R. (1983) Free Energy Coupling within Macromolecules. The Chemical Work of Ligand Binding at the Individual Sites in Cooperative Systems, *J. Mol. Biol. 1*, 223−242.
32. Giangrande, P. H., Kimbrel, E. A., Edwards, D. P., and McDonnell, D. P. (2000) The Opposing Transcriptional Activities of the Two Isoforms of the Human Progesterone Receptor Are Due to Differential Cofactor Binding, *Mol. Cell. Biol. 20*, 3102−3115.
33. Li, Y., Lambert, M. H., and Xu, H. E. (2003) Activation of Nuclear Receptors: A Perspective from Structural Genomics, *Structure 11*, 741−746.
34. Bain, D. L., Franden, M. A., McManaman, J. L., Takimoto, G. S., and Horwitz, K. B. (2000) The N-Terminal Region of the Human Progesterone A-Receptor: Structural Analysis and the Influence of the DNA Binding Domain, *J. Biol. Chem. 275*, 7313−7320.
35. Bain, D. L., Franden, M. A., McManaman, J. L., Takimoto, G. S., and Horwitz, K. B. (2001) The N-Terminal Region of Human Progesterone B-Receptors: Biophysical and Biochemical Comparison to A-Receptors, *J. Biol. Chem. 276*, 23825−23831.
36. Beckett, D. (2001) Regulated Assembly of Transcription Factors and Control of Transcription Initiation, *J. Mol. Biol. 314*, 335−352.
37. Senear, D. F., Ross, J. B., and Laue, T. M. (1998) Analysis of Protein and DNA-Mediated Contributions to Cooperative Assembly of Protein-DNA Complexes, *Methods 16*, 3−20.
38. Ptashne, M. (1986) *A Genetic Switch: Gene Control and Phage Lambda*, Cell Press and Blackwell Scientific Publications.
39. Anzick, S. L., Kononen, J., Walker, R. L., Azorsa, D. O., Tanner, M. M., Guan, X.-Y., Sauter, G., Kallioniemi, O.-P., Trent, J. M., and Meltzer, P. S. (1997) AIB1, a Steroid Receptor Coactivator Amplified in Breast and Ovarian Cancer, *Science 277*, 965−968.
40. Bevington, P. R., and Robinson, D. K. (1969) *Data Reduction and Error Analysis for the Physical Sciences*, 3rd ed., McGraw-Hill Higher Education.

BI700850V